Evaluation of Peripheral Vascular Disease Using Optical Tomography

Alessandro G. Smeraldi[4], Nelson A. Franco[1], Rosemarie E. Hardin[1], Michael S. Katz[1], David P. Klemer[2], Harry L. Graber[2], Christoph H. Schmitz[2], MaryAnn Banerji[3], Thomas F. Panetta[4] and Randall L. Barbour[2]

Departments of Surgery[1],Pathology[2] and Medicine[3], SUNY Downstate Medical Center, 450 Clarkson Avenue, Brooklyn, New York 11203

Department of Vascular Surgery[4], Staten Island University Hospital, 475 Seaview Avenue, Staten Island, New York 10305

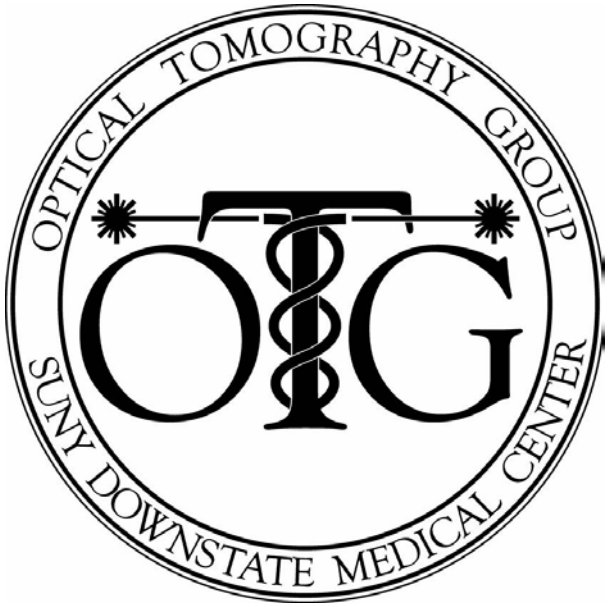

Evaluation of Peripheral Vascular Disease Using Optical Tomography

INTRODUCTION

We have previously examined the microvascular reactivity to a cuff occlusion provocation. The cuff occlusion provocation isolates responses to the vascular tree. In this study, we seek to understand the vascular-tissue coupling through a similar provocation. The provocation we used is arterial occlusion. By inducing ischemia in the tissue of euglycemic and diabetic volunteers, we hope see if DYNOT measurements can discriminate healthy and diseased tissue states.

This suggests the possibility of eventually replacing the invasive clinical test performed at present with a DYNOT-based noninvasive imaging technique. As a general matter, clinical adoption of near-infrared optical techniques in diabetes management would offer significant advantages over conventional approaches: (1) measurements are done in real time, (2) they are noninvasive, and (3) they may obviate the need for multiple repeated blood draws.

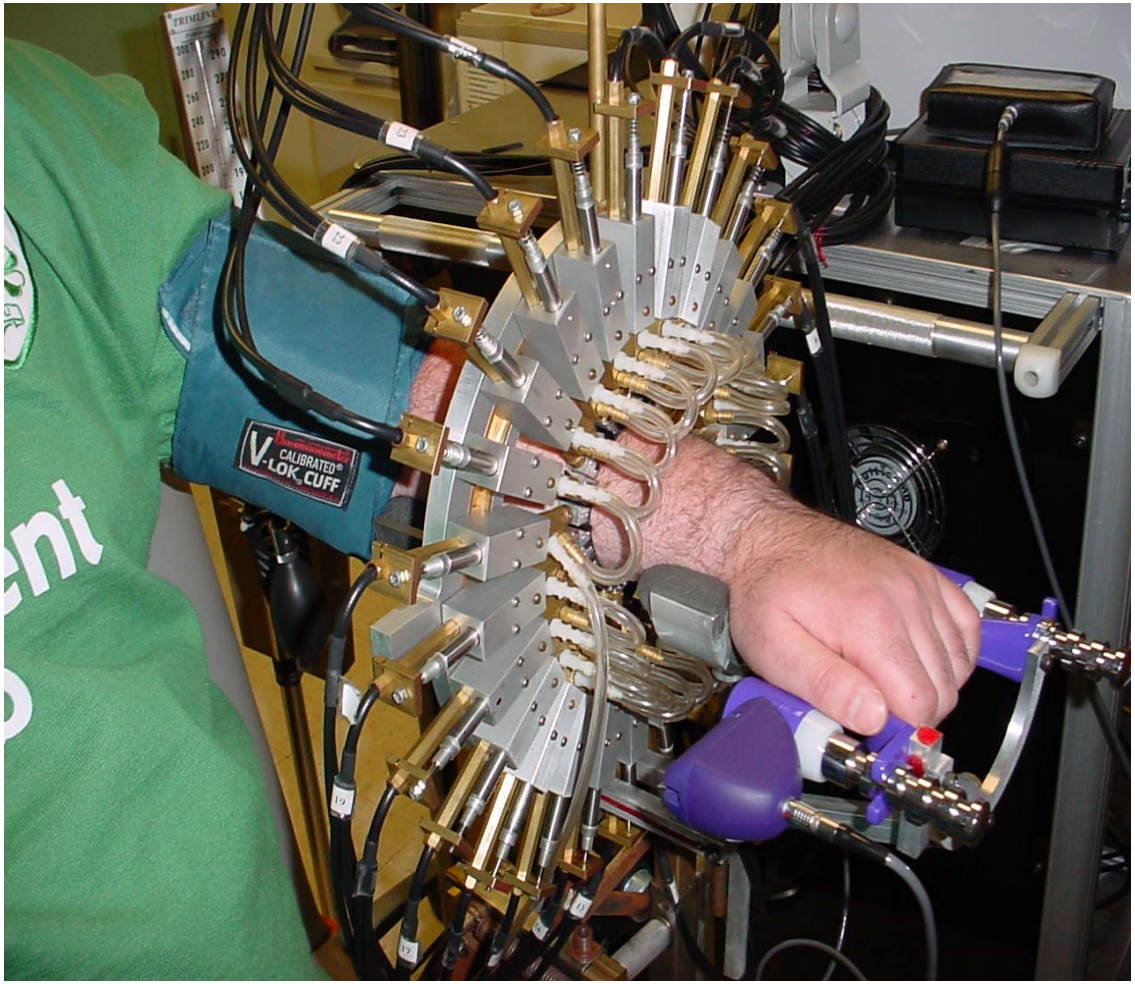

Figure 1

Detector Position and Setup

Typical placement of volunteer's arm in the Iris Imaging Head and placement of BP Cuff for venous occlusion provocation.

METHODS

Fourteen volunteers were measured; 20% were female, 40% were ethnic minorities. Volunteer ages ranged from 18 to 62. Five of the volunteers were clinically diagnosed, poorly to moderately-controlled diabetics receiving only oral therapy ($HbA1_C$ <9%). Patients diagnosed as diabetics had a duration of diagnosis greater than 5 years.

The volunteer was attached to the following monitors: 3 Lead EKG, Pulse Oximeter, Blood Pressure Cuff, and Radial Artery Tonometer. The volunteer was then placed in a seated recumbent position and remained at rest during the measurements. The volunteer was allowed to acclimate to his/her position in the chair and the environment for twenty minutes before any experimental provocations were initiated. Measurements were obtained from a dual-wavelength (760nm and 830nm) optical tomographic iris measurement head (Figure 1) positioned around the left prone forearm.

Experimental provocations consisted of inflation of a blood pressure cuff positioned around the left arm to a pressure of 180 mmHg to produce arterial occlusion and induce tissue ischemia. This provocation was performed 4 times. The provocation lasted 60, 120, 240 and 360 seconds with 400 seconds between each provocation. Figure 2 illustrates the three phases of this provocation.

Data Analysis

Once measurements were acquired, the data was processed with the *dyna*LYZE software package.

1. Data pre-processing. Raw data for all channels that passed the data-integrity checks were normalized based on the time-varying laser intensity recorded during the experiment, then were further normalized based on the mean value recorded during the baseline period. During this step, an adaptive median filtering algorithm was applied, as needed, to eliminate negative instantaneous values resulting from measurement noise.

2. Image Reconstruction. Image recovery was achieved using the Normalized Difference Method [2]. As previously shown, this algorithm is markedly insensitive to expected uncertainties in boundary conditions, which are unavoidable in experimental methods. A truncated singular value decomposition procedure is used to solve the linear perturbation equation. The absorption coefficient images were subsequently post-processed to produce image time series for oxygenated, deoxygenated, and total hemoglobin (Hb) concentration changes. For the reconstructed image time series, the changes in Hb concentration (Fig. 2) were computed from the reconstructed two-wavelength absorption coefficients at each FEM mesh node, by solving a simple algebraic system of two equations in two unknowns. For the detector readings time series, relative concentration changes for the Hb states were estimated via a modified Lambert-Beer law.

3. Signal Analysis. 1) A general linear model (GLM) algorithm was applied to the detector data or the image time series to find the best fit of each time series to a model function created by spatially averaging over all source-detector pairs or, in the case of reconstructed images, over all pixels in each image. The GLM method is schematically illustrated in Fig. 3. The analysis yields the fitting parameters (GLM coefficients) for each data channel or image pixel, as well as the percentage of variance accounted for (PVA) in each channel's or FEM mesh node's time series. 2) A rate analysis strategy was employed to quantify changes in vascular compliance by judging the transient response of the optical signal to the occlusion maneuver in absence and presence of a heating stimulus. This analysis employed measures of the steepness in the transient rise ("upslope") and fall ("downslope") of the optical signal, as well as the temporal width of the signal response. In addition, the integrated area under the signal curve during the response interval was used as a measure of the response strength.

Progression of Ischemia

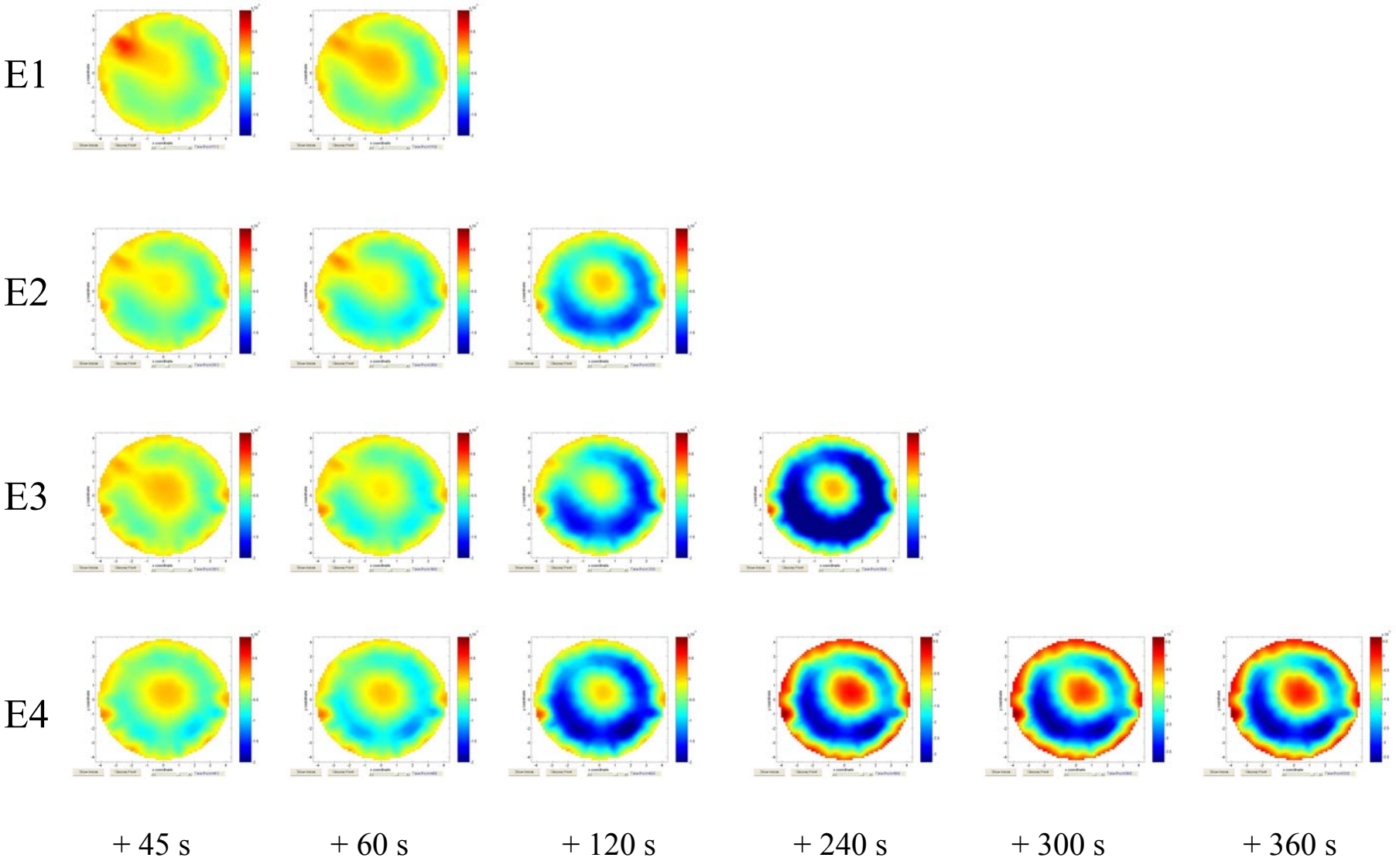

Figure 5

Oxy-Hemoglobin (Euglycemic)

Progression of Ischemia

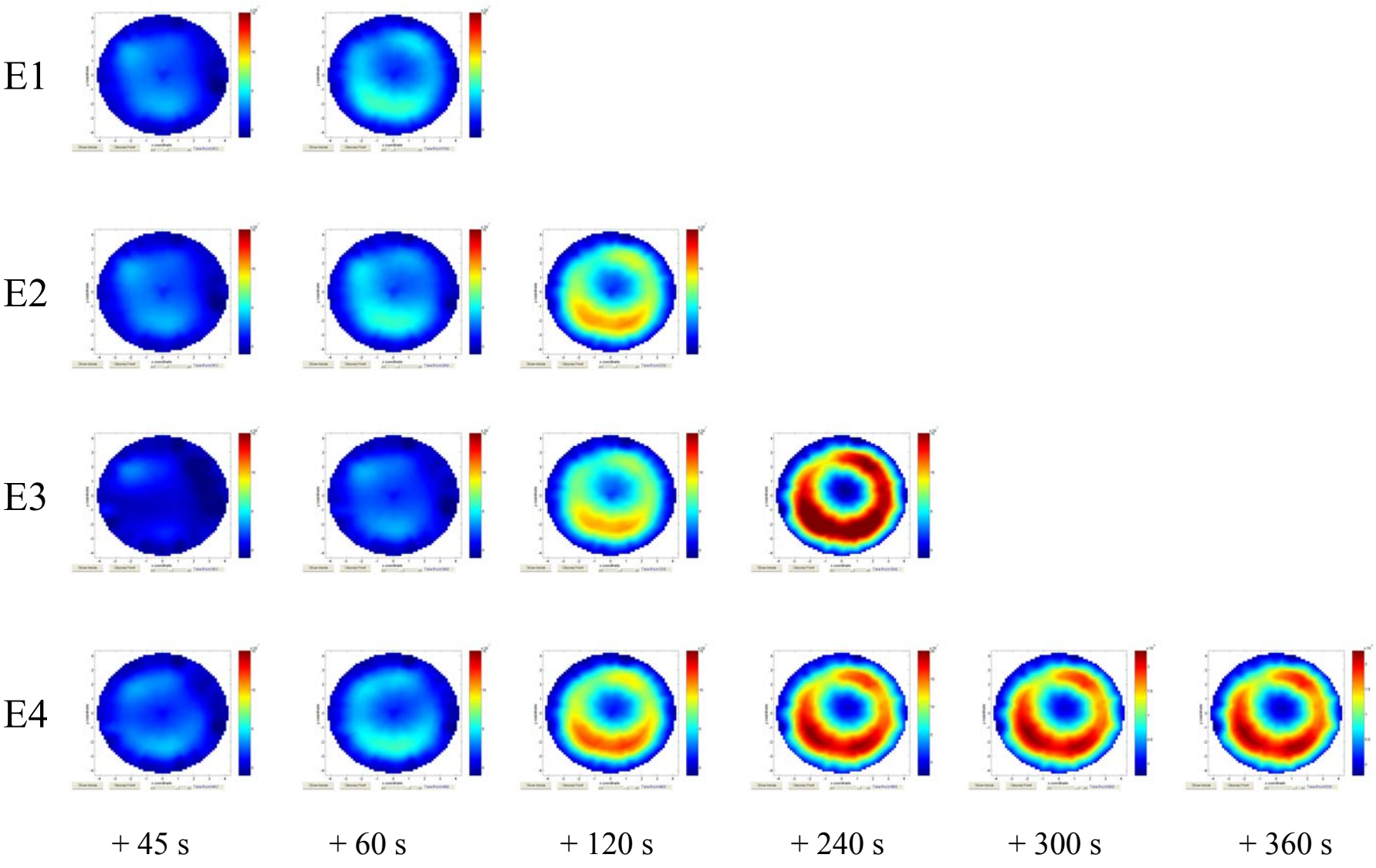

Figure 6

Deoxy-Hemoglobin (Euglycemic)

Progression of Ischemia

Figures 5 and 6 shows the dynamic changes seen in the image time series of Oxy and Deoxy-Hemoglobin in the progression of ischemia in a euglycemic volunteer. The increased reactivity and intensity seen in the lower half of the image corresponds to the location of the flexor muscle bellies of the forearm.

Figures 7 and 8 also follow the progression of ischemia in a poorly controlled diabetic volunteer. The dynamic changes previously seen are not apparent in this volunteer.

It is a known clinical finding that the poorly controlled diabetic is prone to severe peripheral vascular disease and tissue loss [6,7]. This series of images demonstrates that the tissue of the diabetic is already in a state of mild ischemia and is less reactive to ischemic conditions.

Progression of Ischemia

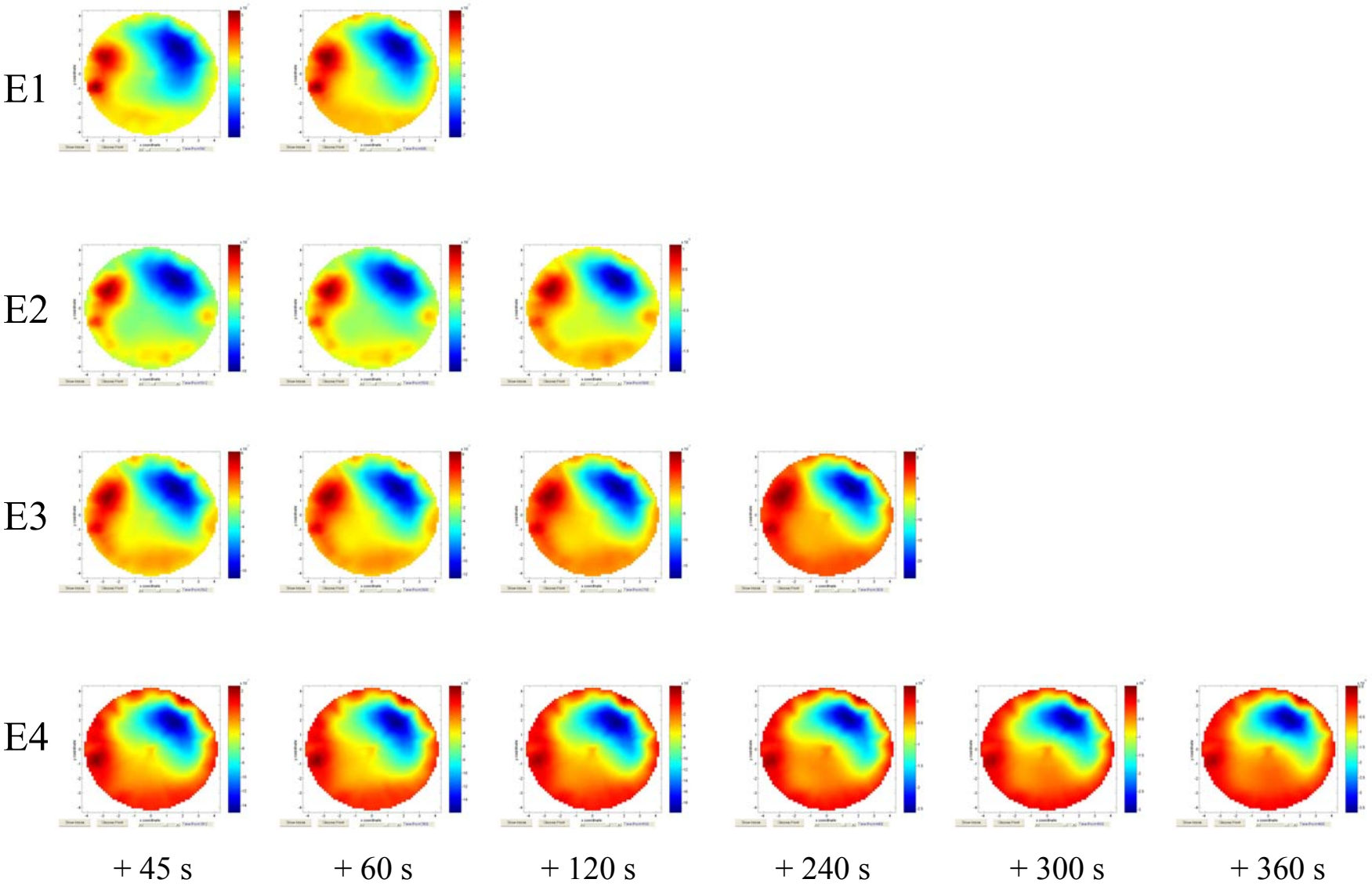

Figure 7

Oxy-Hemoglobin (Diabetic)

Progression of Ischemia

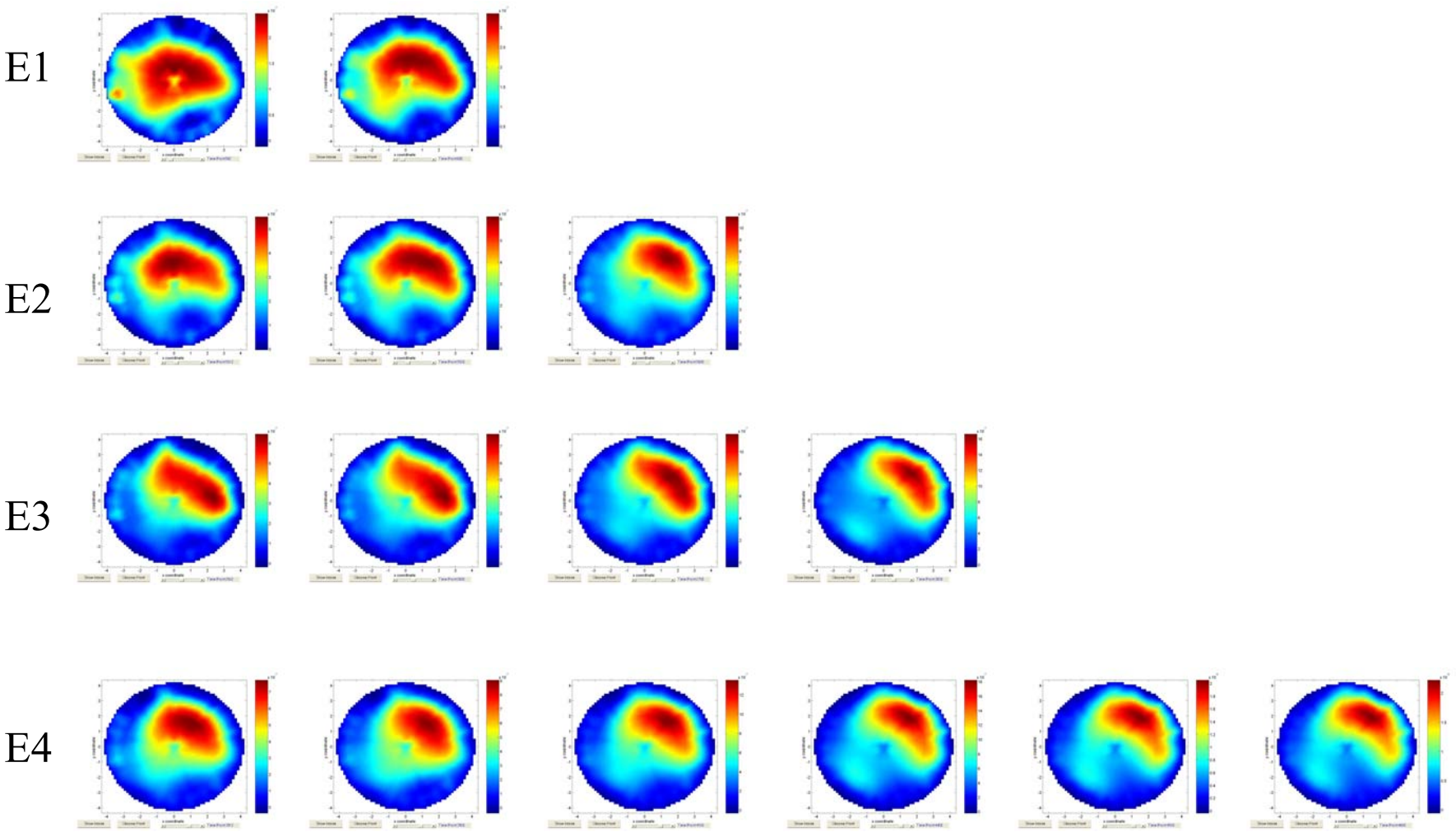

Figure 8

Deoxy-Hemoglobin (Diabetic)

Deoxy-Hemoglobin (Euglycemic)

Phase I Up Slope

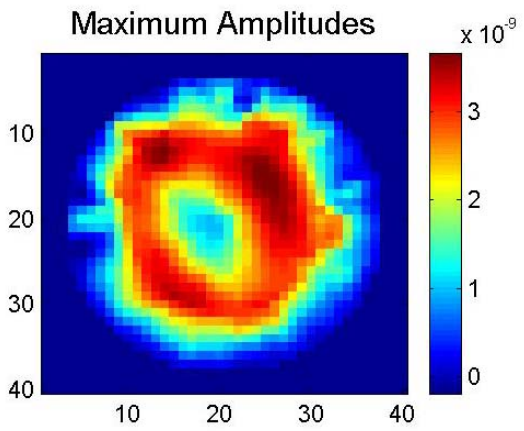

1 min

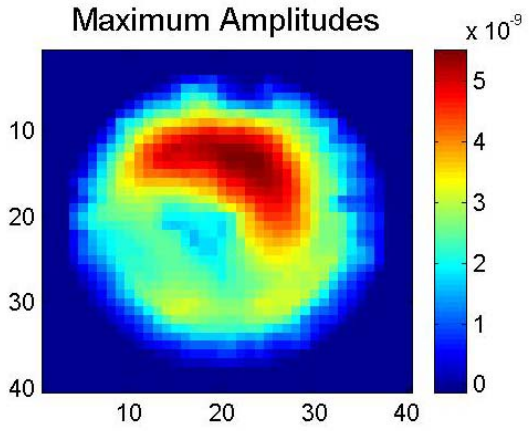

2 min

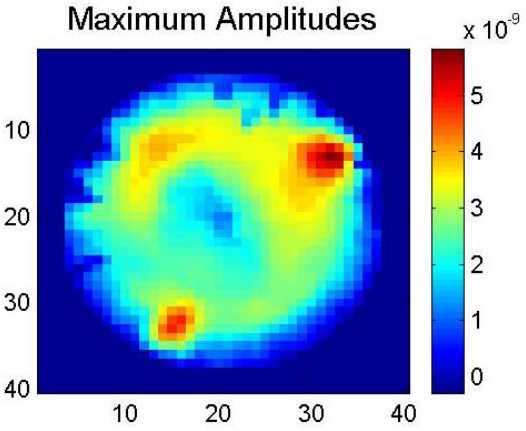

4 mın

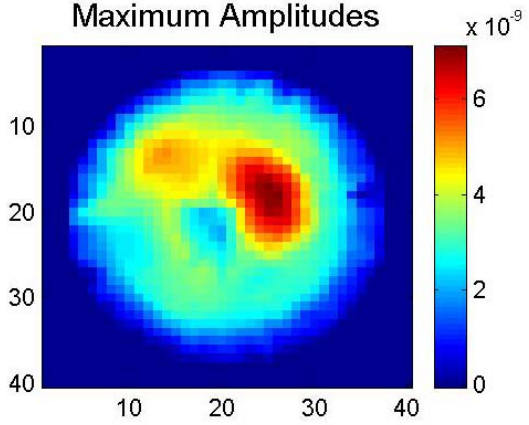

6 min

Deoxy-Hemoglobin (Diabetic)

Phase I Up Slope

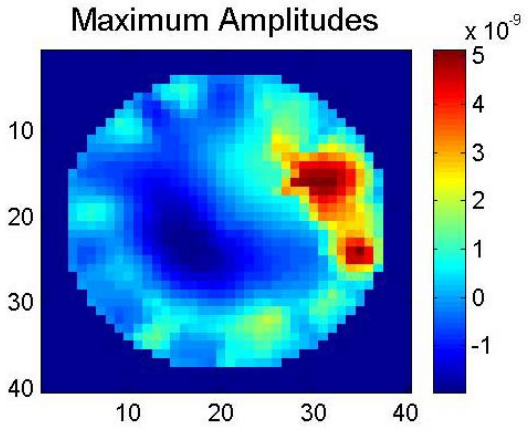

1 min

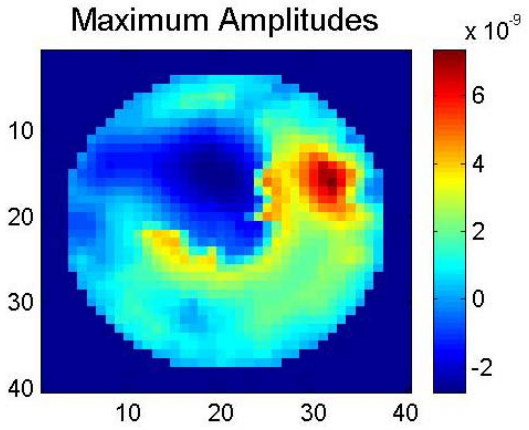

2 min

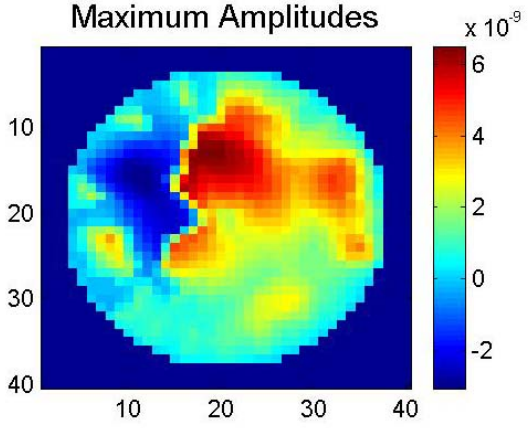

4 min

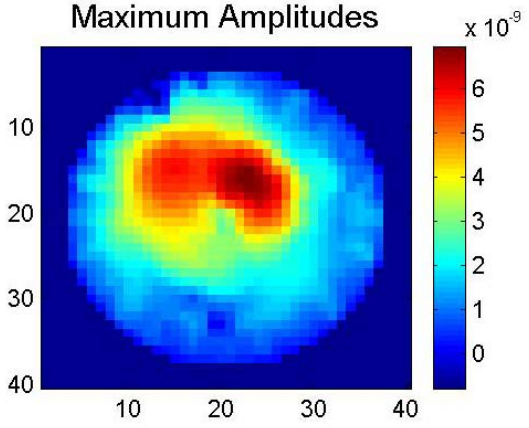

6 min

Oxy-Hemoglobin (Euglycemic)

Phase I Down Slope

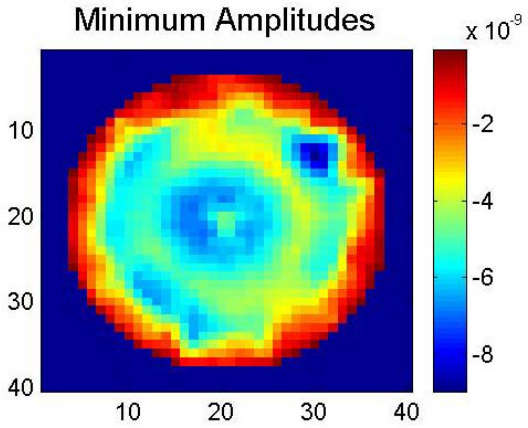

1 min

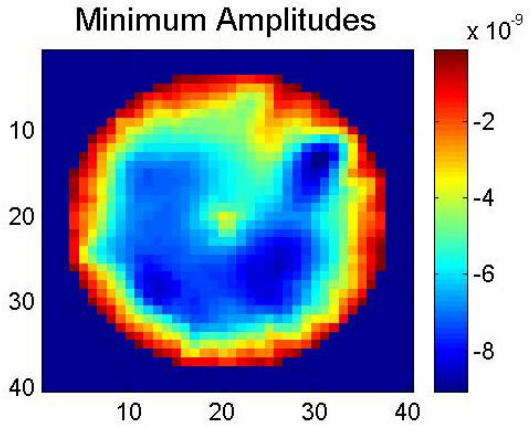

2 min

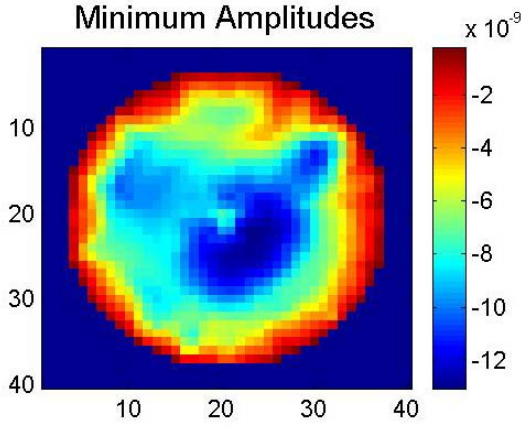

4 min

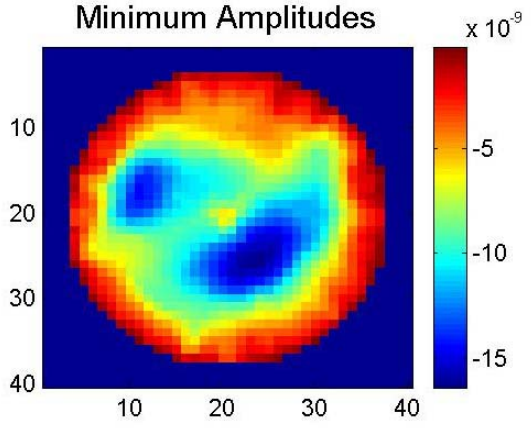

6 min

Oxy-Hemoglobin (Diabetic)

Phase I Down Slope

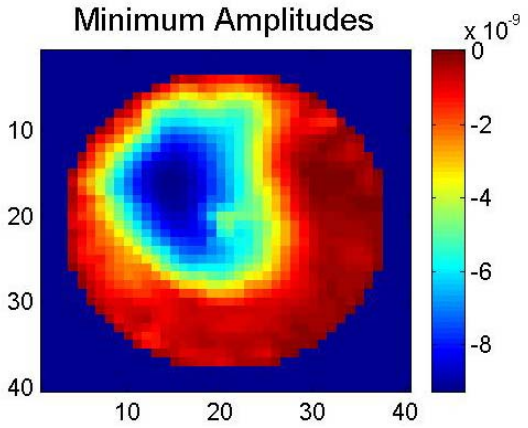

1 min

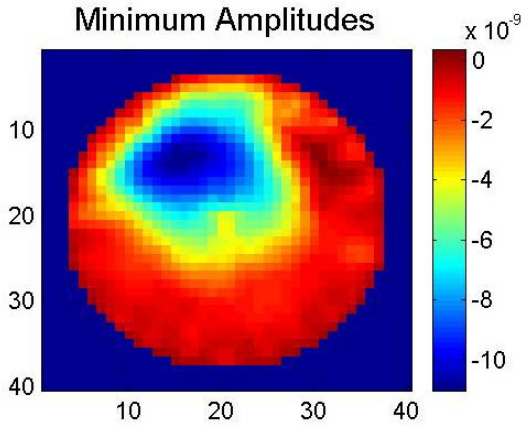

2 min

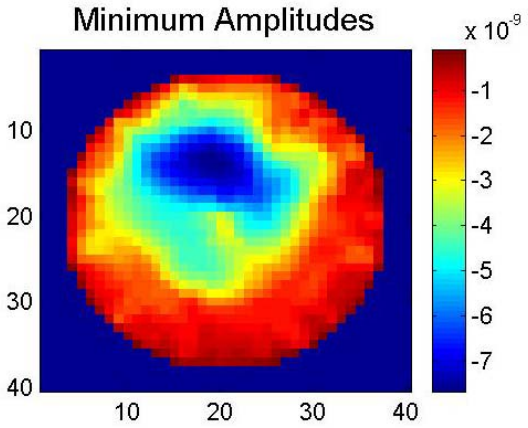

4 min

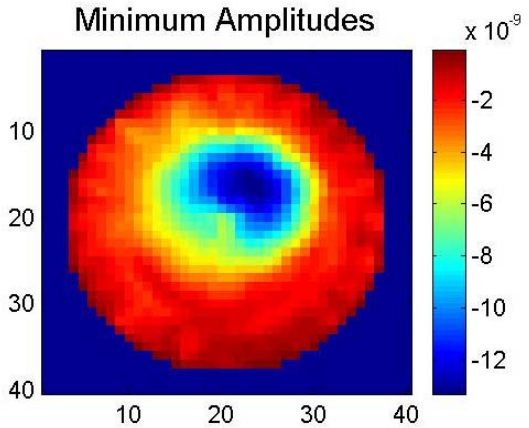

6 min

Oxy-Hemoglobin (Diabetic)

Phase I Down Slope

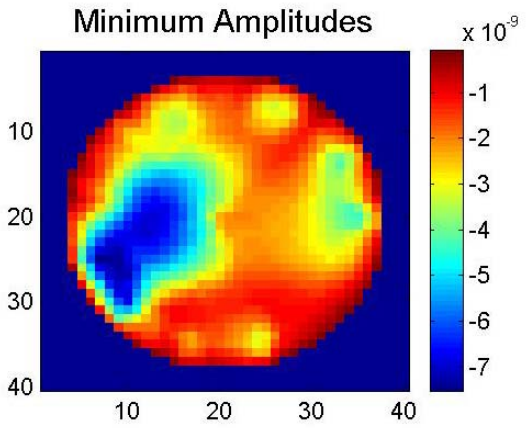

1 min

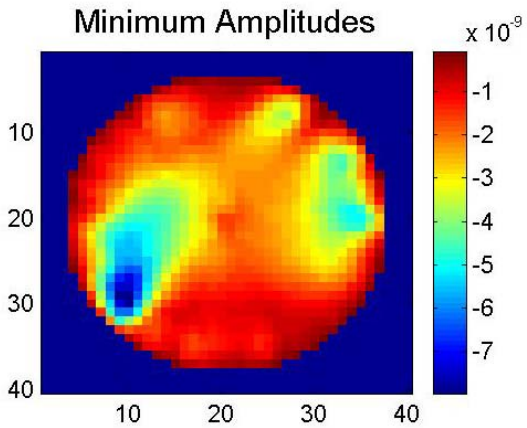

2 min

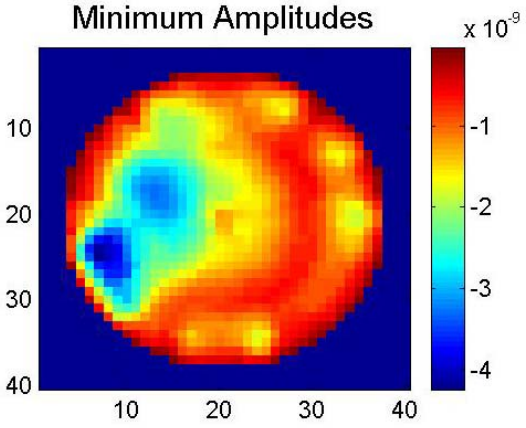

4 min

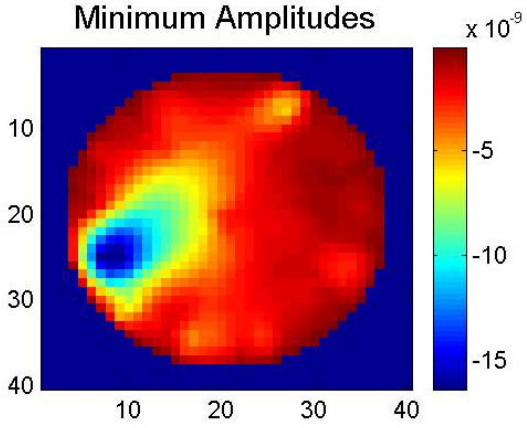

6 min

Deoxy-Hemoglobin (Diabetic)

Phase II Down Slope

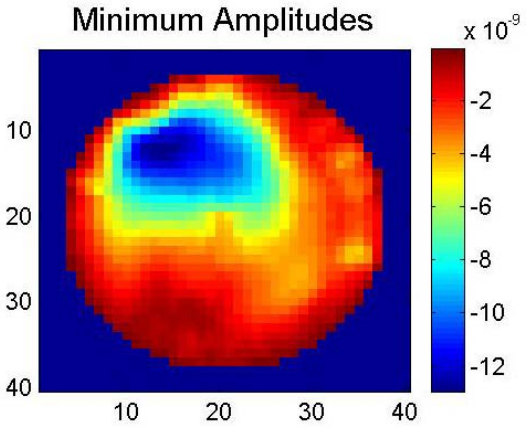

1 min

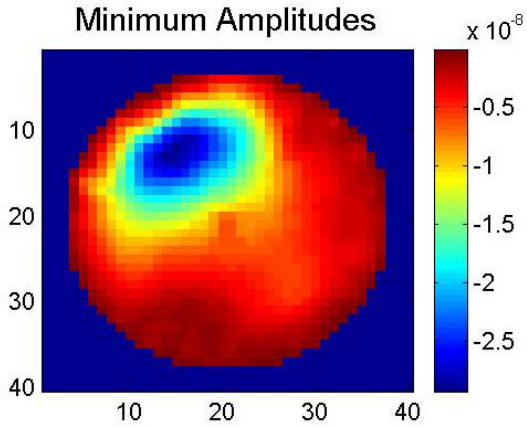

2 min

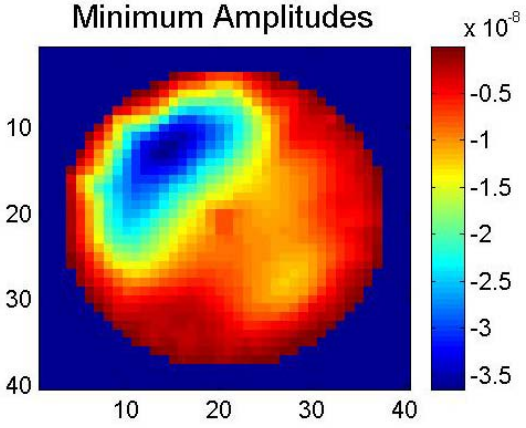

4 min

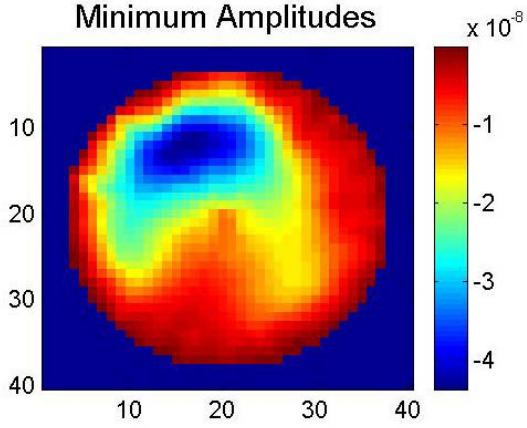

6 min

Deoxy-Hemoglobin (Diabetic)

Phase II Down Slope

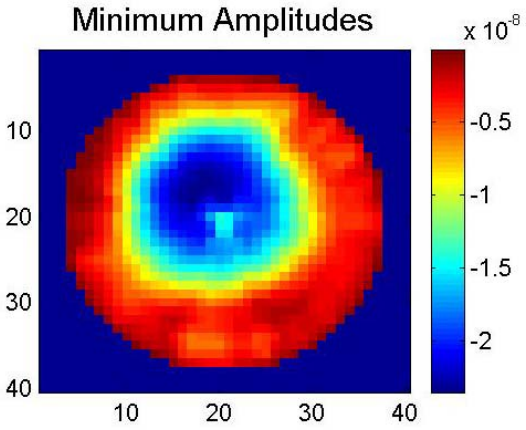

1 min

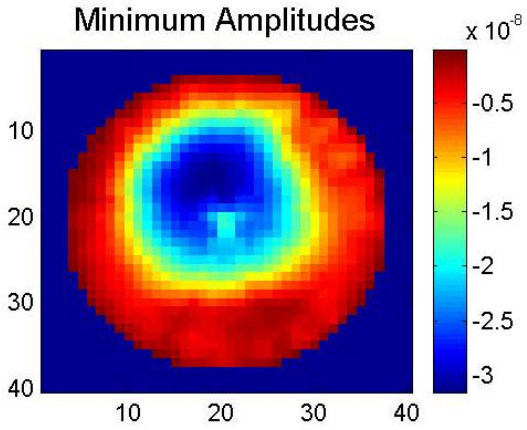

2 min

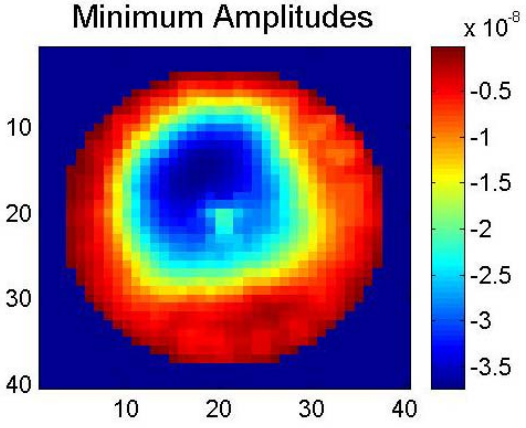

4 min

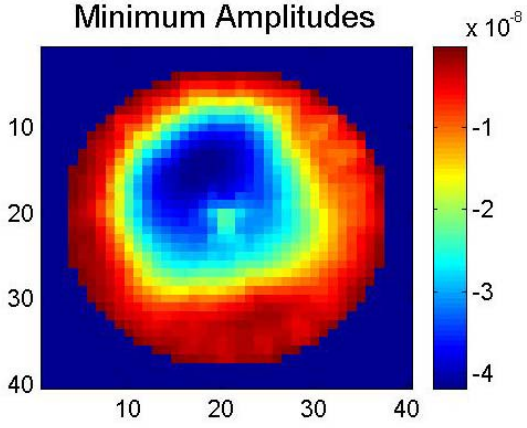

6 min

Deoxy-Hemoglobin (Euglycemic)

Phase II Up Slope

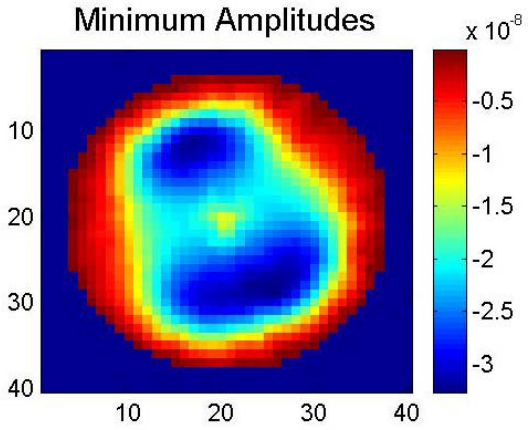

1 min

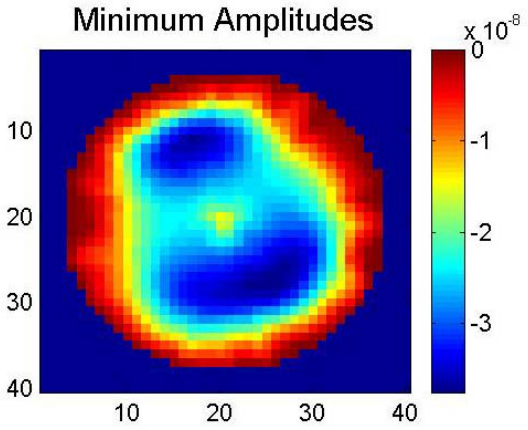

2 min

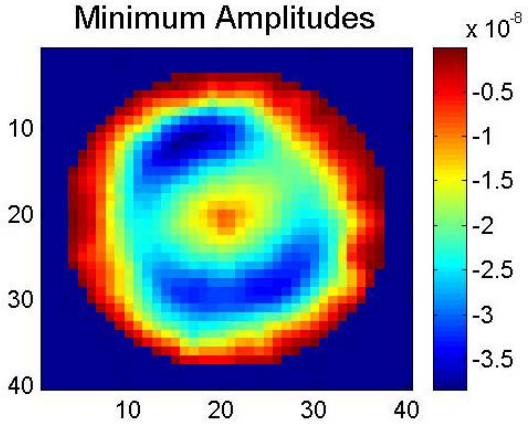

4 min

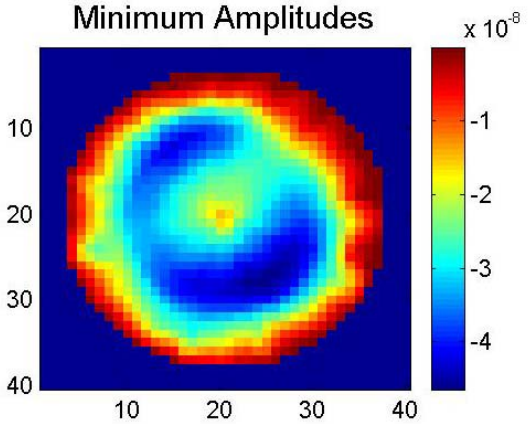

6 min

Deoxy-Hemoglobin (Euglycemic)

Phase II Down Slope

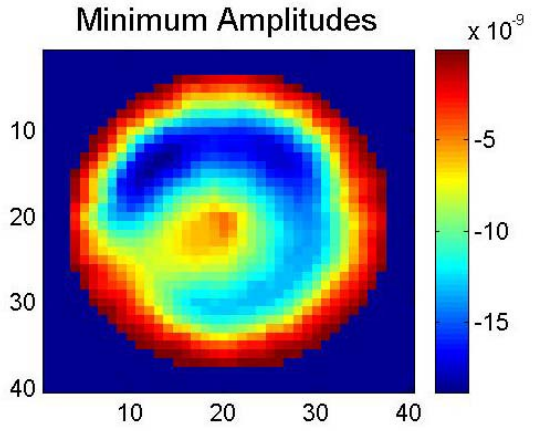

1 min

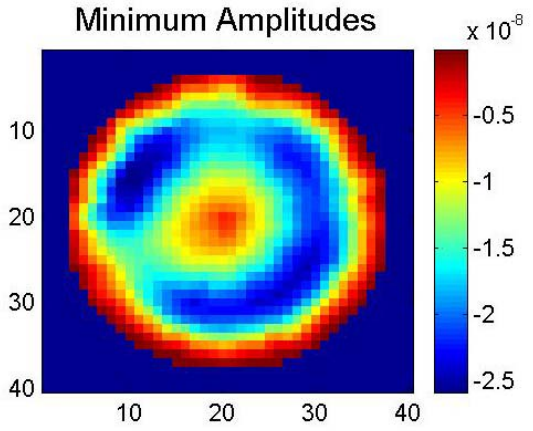

2 min

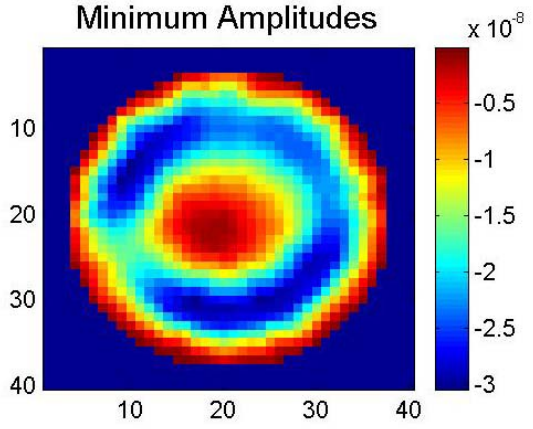

4 min

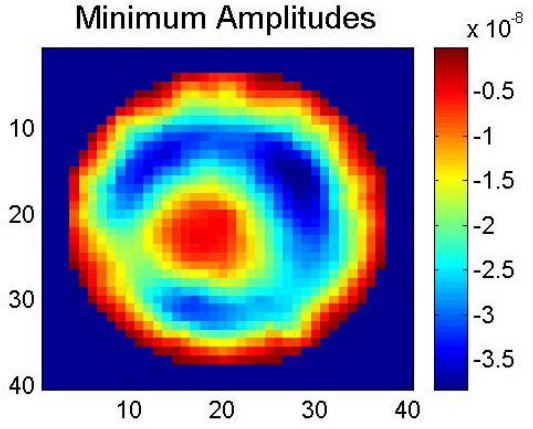

6 min

Oxy-Hemoglobin (Euglycemic)

Phase II Up Slope

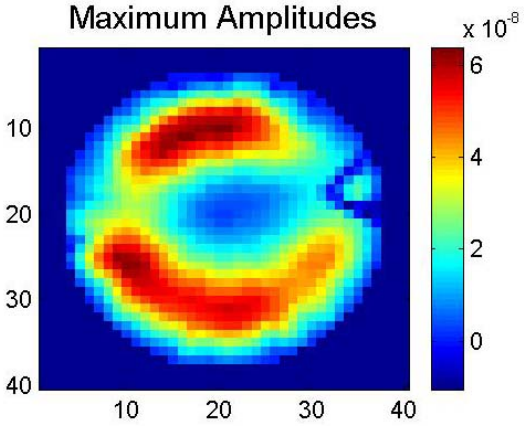

1 min

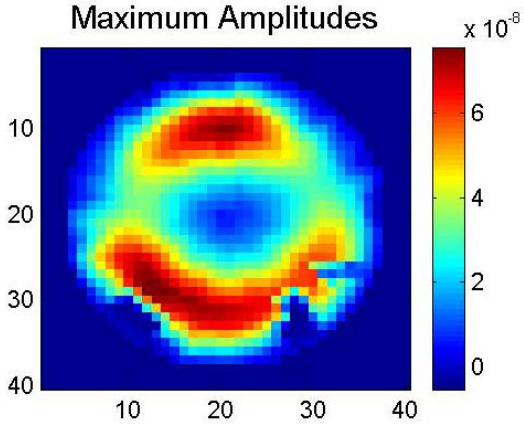

2 min

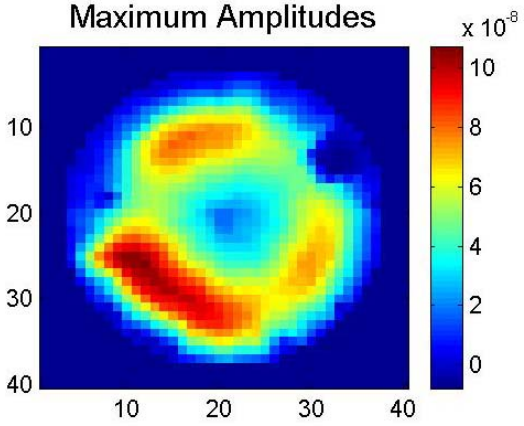

4 min

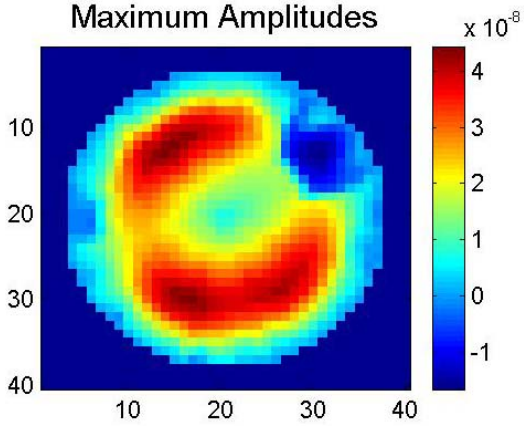

6 min

Oxy-Hemoglobin (Diabetic)

Phase II Up Slope

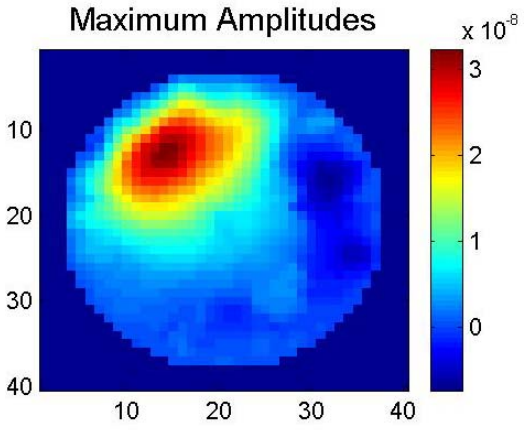

1 min

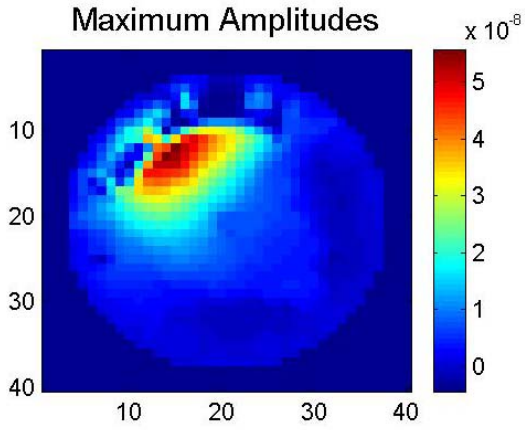

2 min

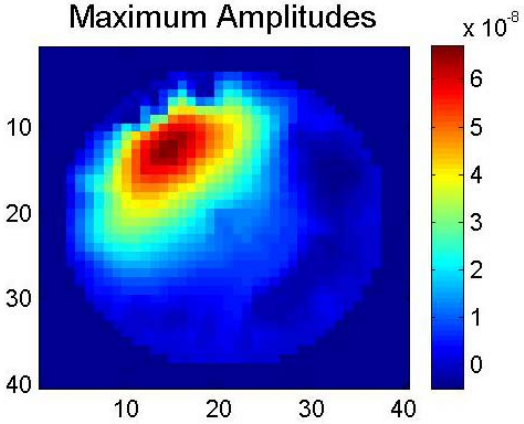

4 min

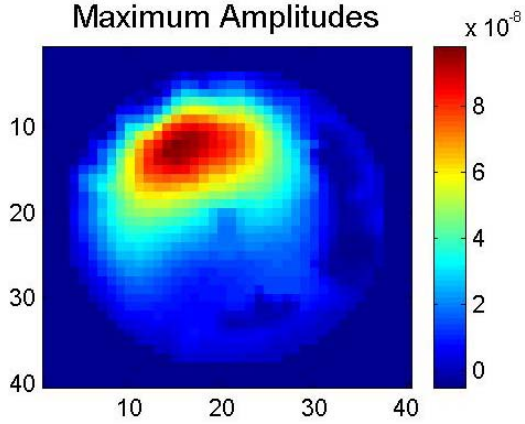

6 min

Oxy-Hemoglobin (Euglycemic)

Phase III Down Slope

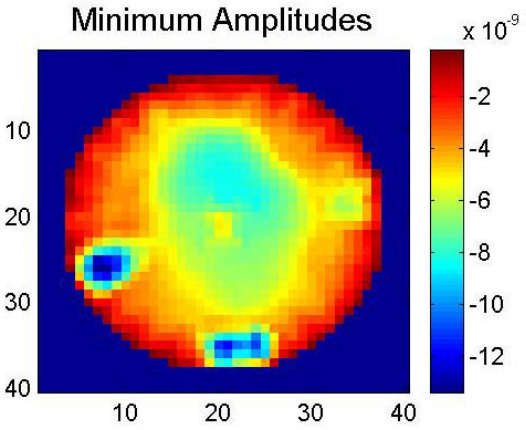

1 min

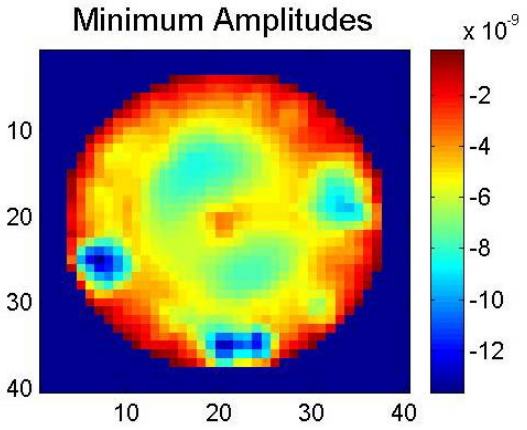

2 min

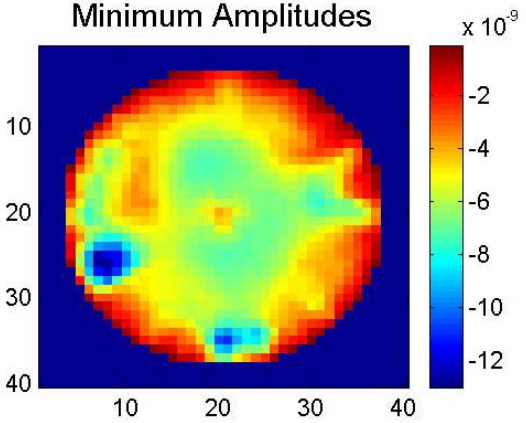

4 min

Oxy-Hemoglobin (Diabetic)

Phase III Down Slope

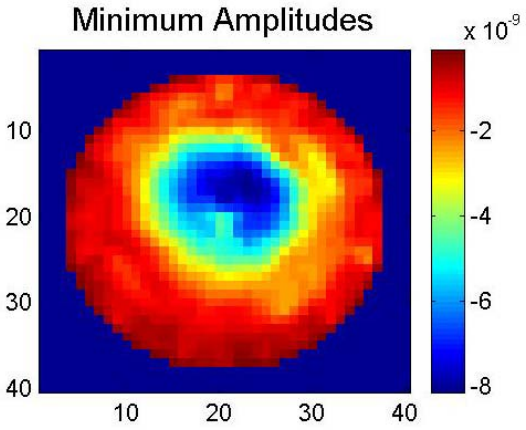

1 min

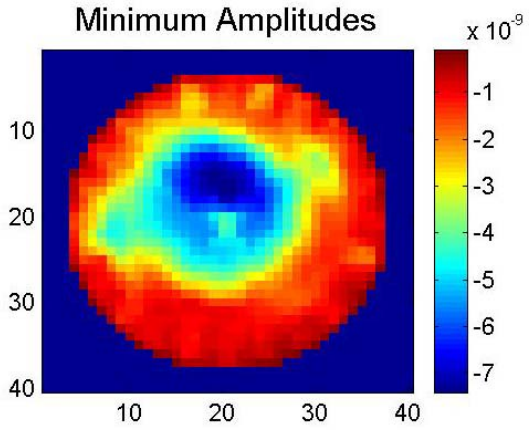

2 min

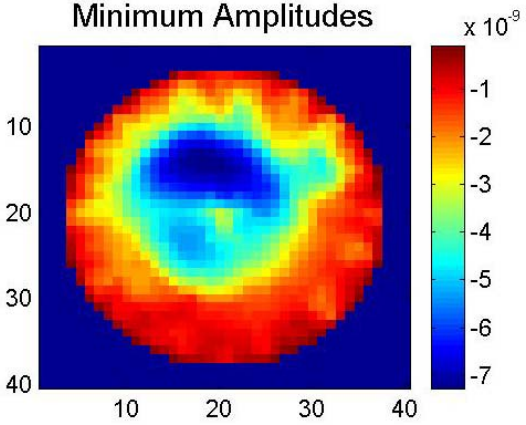

4 min

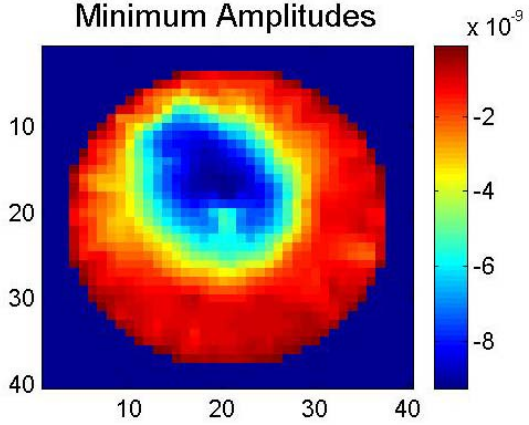

6 min

Deoxy-Hemoglobin (Euglycemic)

Phase III Up Slope

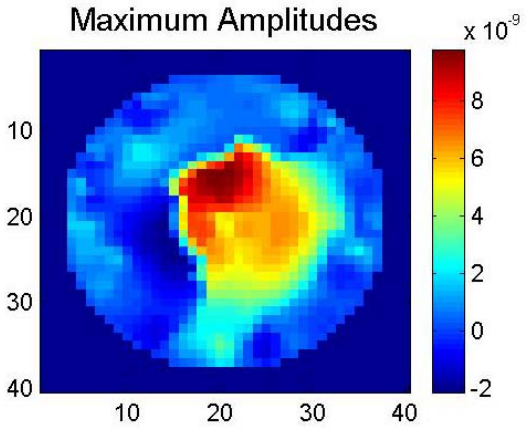

1 min

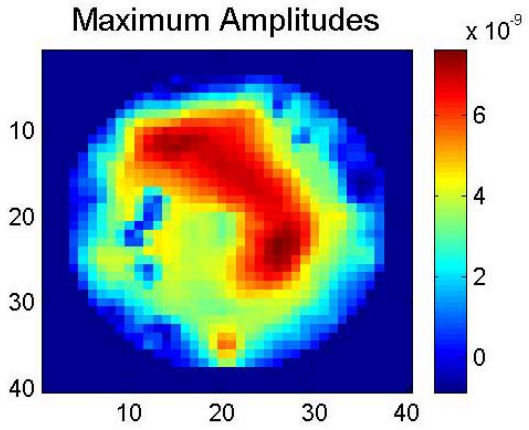

2 min

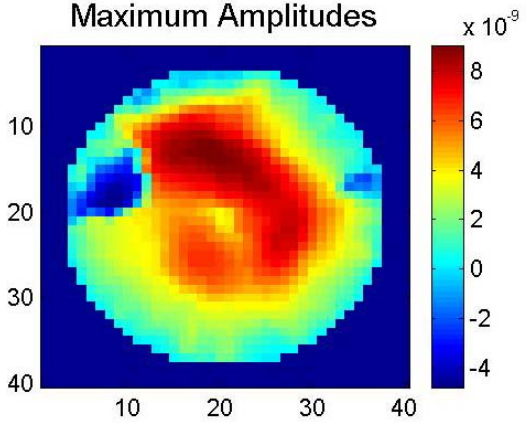

4 min

Deoxy-Hemoglobin (Diabetic)

Phase III Up Slope

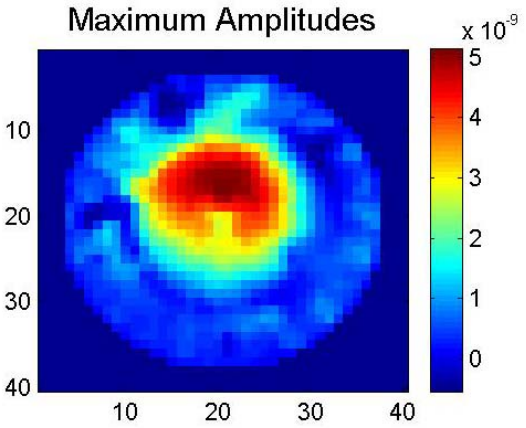

1 min

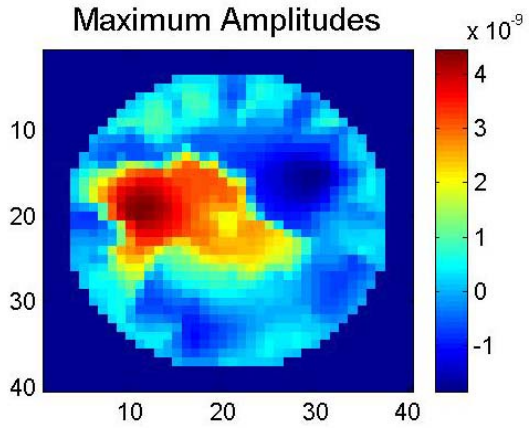

2 min

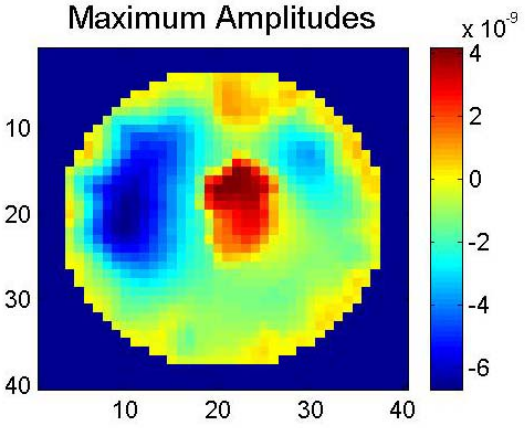

4 min

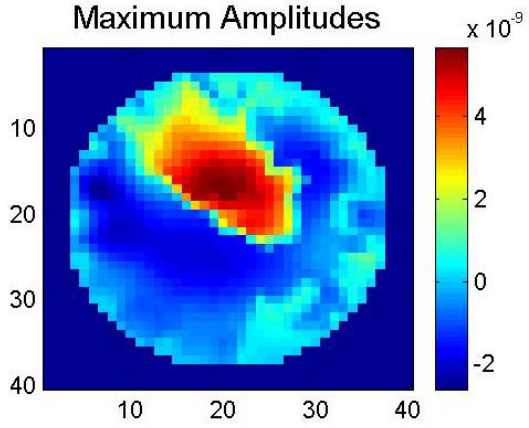

6 min

Oxy-Hemoglobin (Euglycemic)

GLM Images

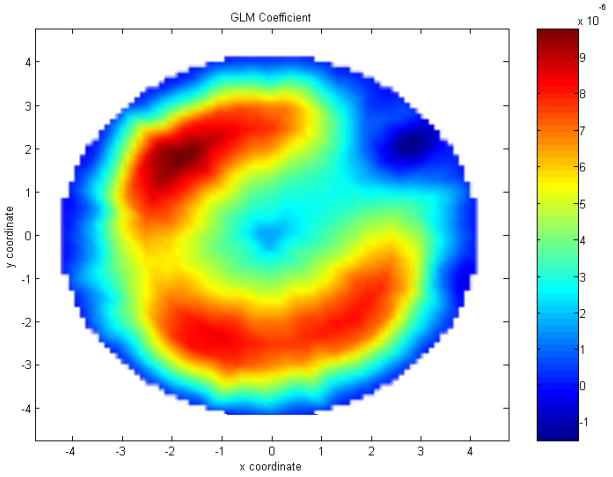

1 min

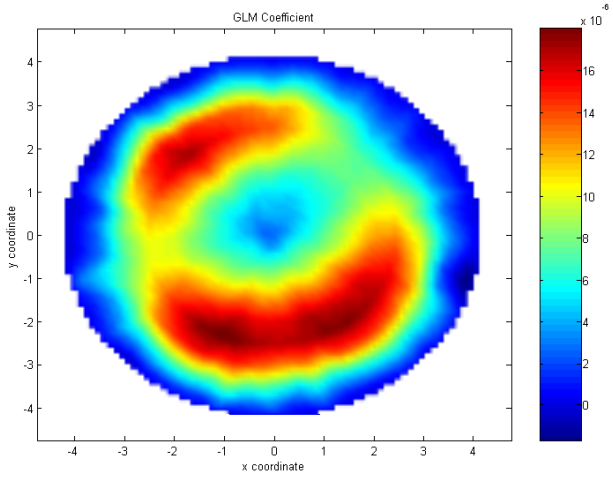

2 min

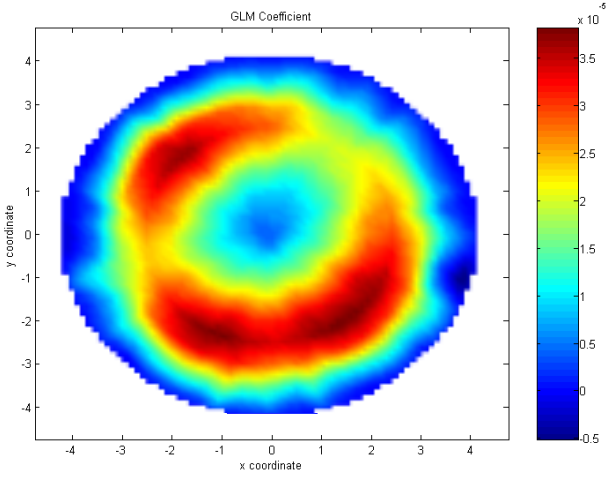

4 min

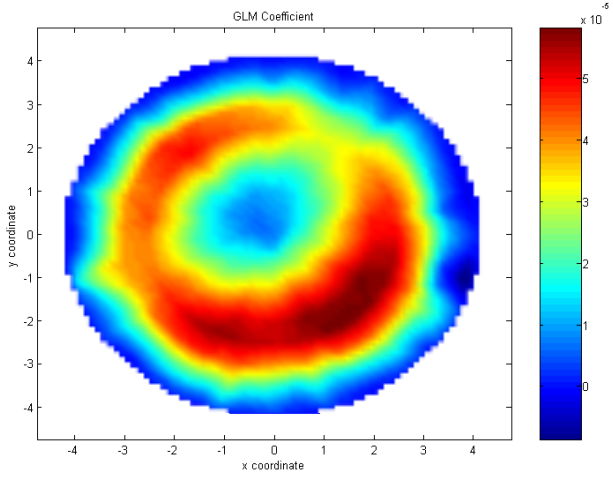

6 min

Deoxy-Hemoglobin (Euglycemic)

GLM Images

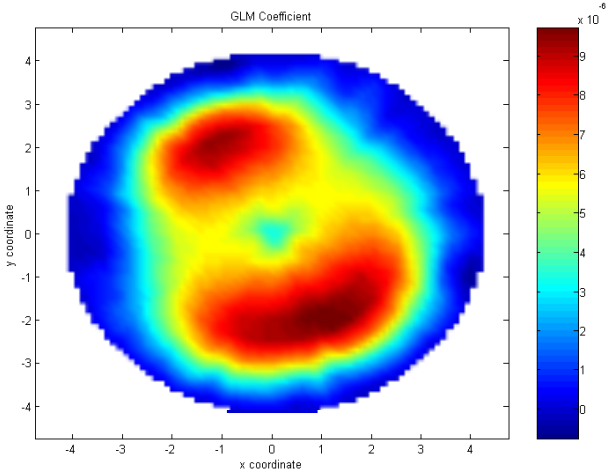

1 min

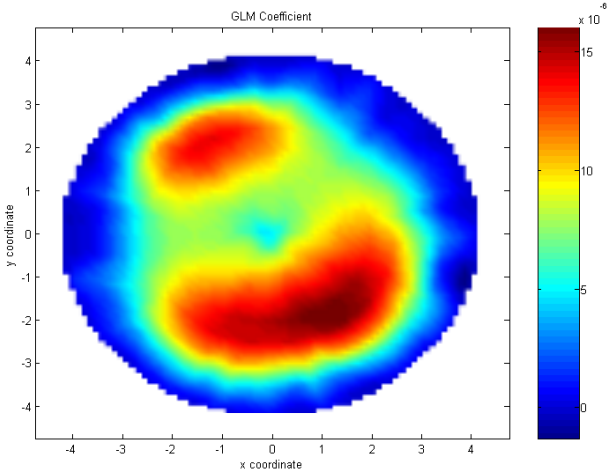

2 min

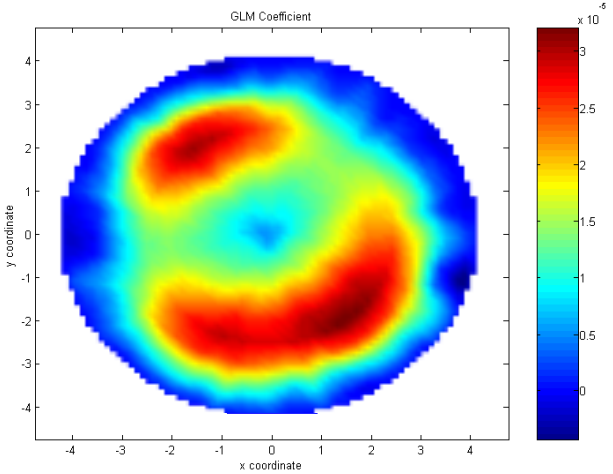

4 min

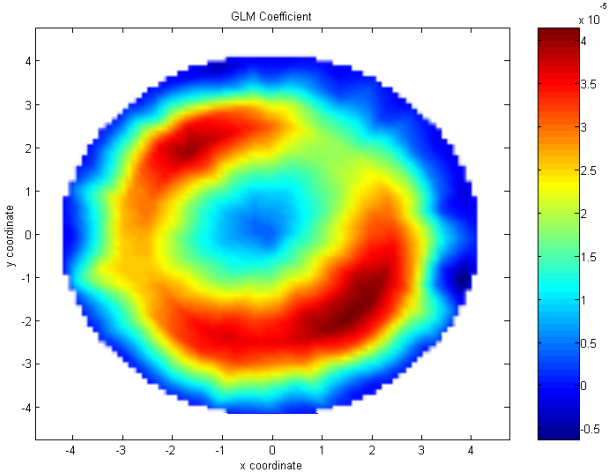

6 min

Deoxy-Hemoglobin (Diabetic)

GLM Images

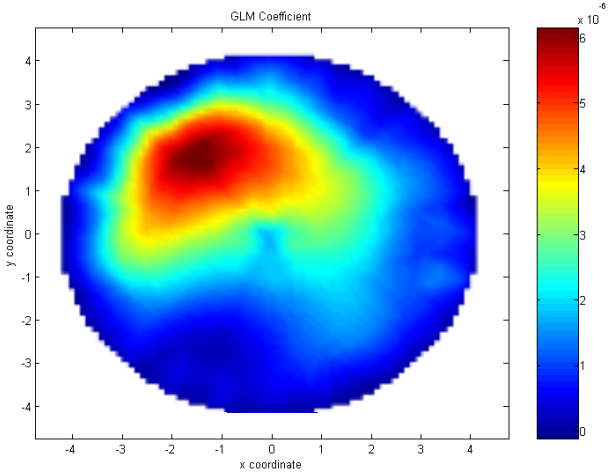

1 min

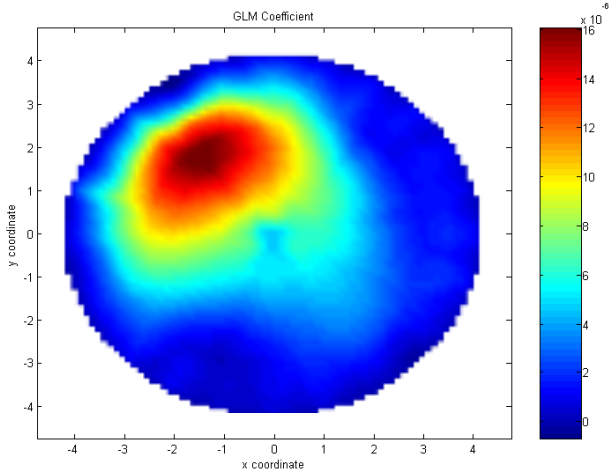

2 min

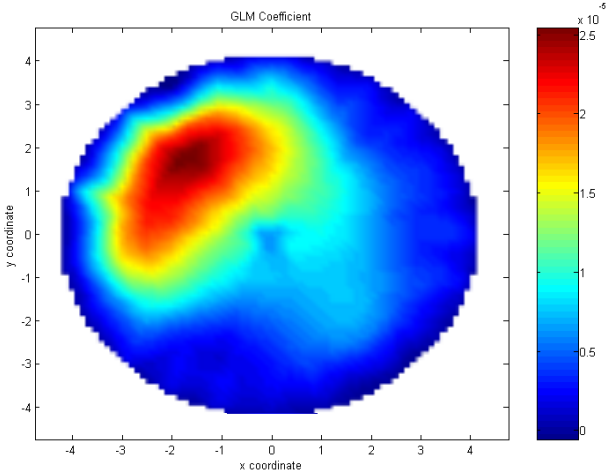

4 min

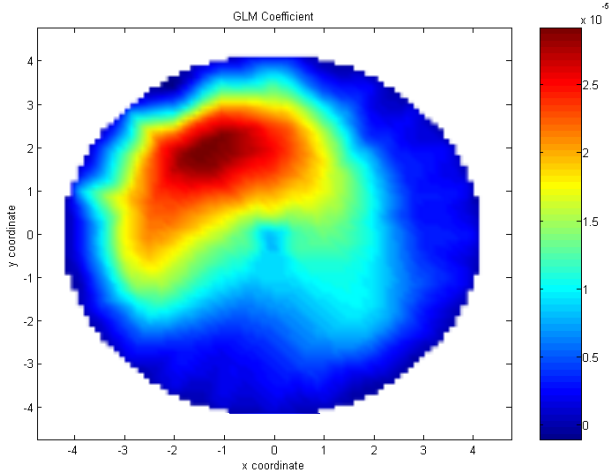

6 min

Oxy-Hemoglobin (Diabetic)

GLM Images

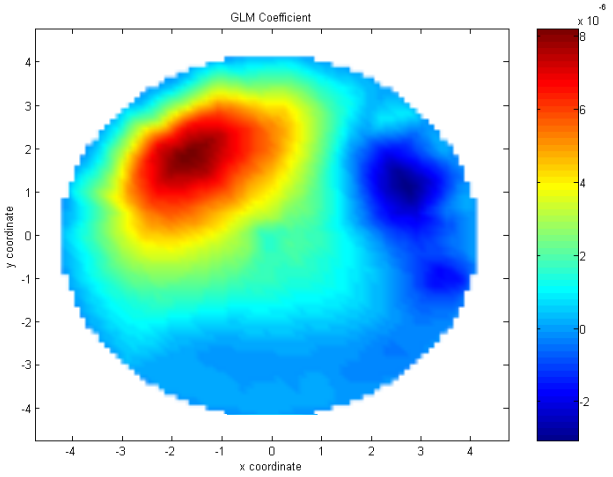

1 min

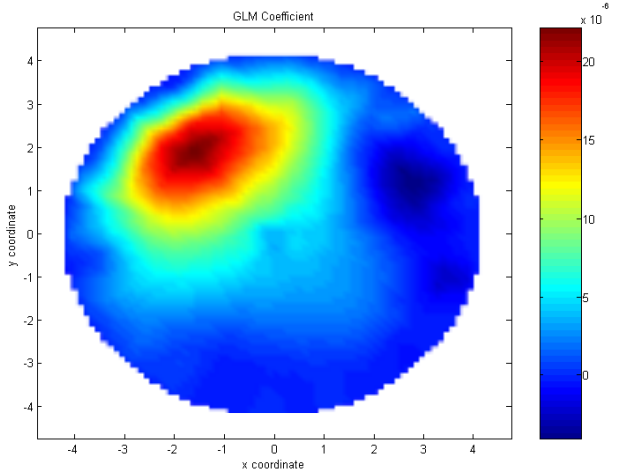

2 min

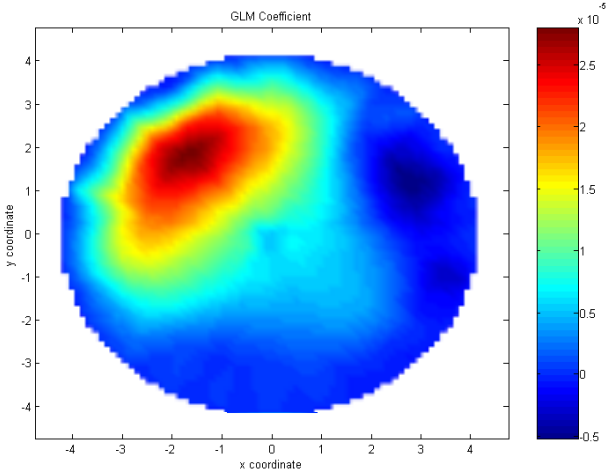

4 min

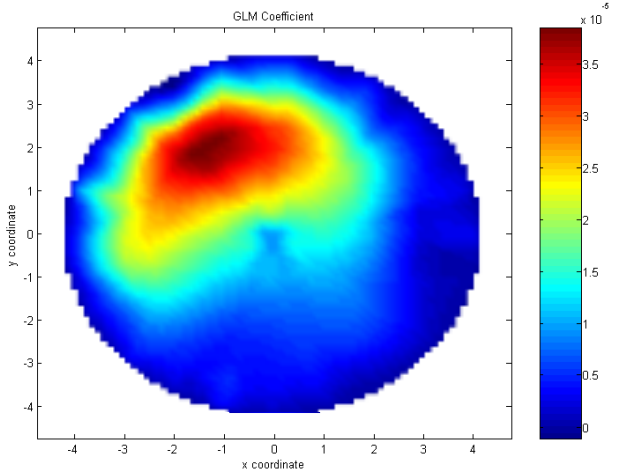

6 min

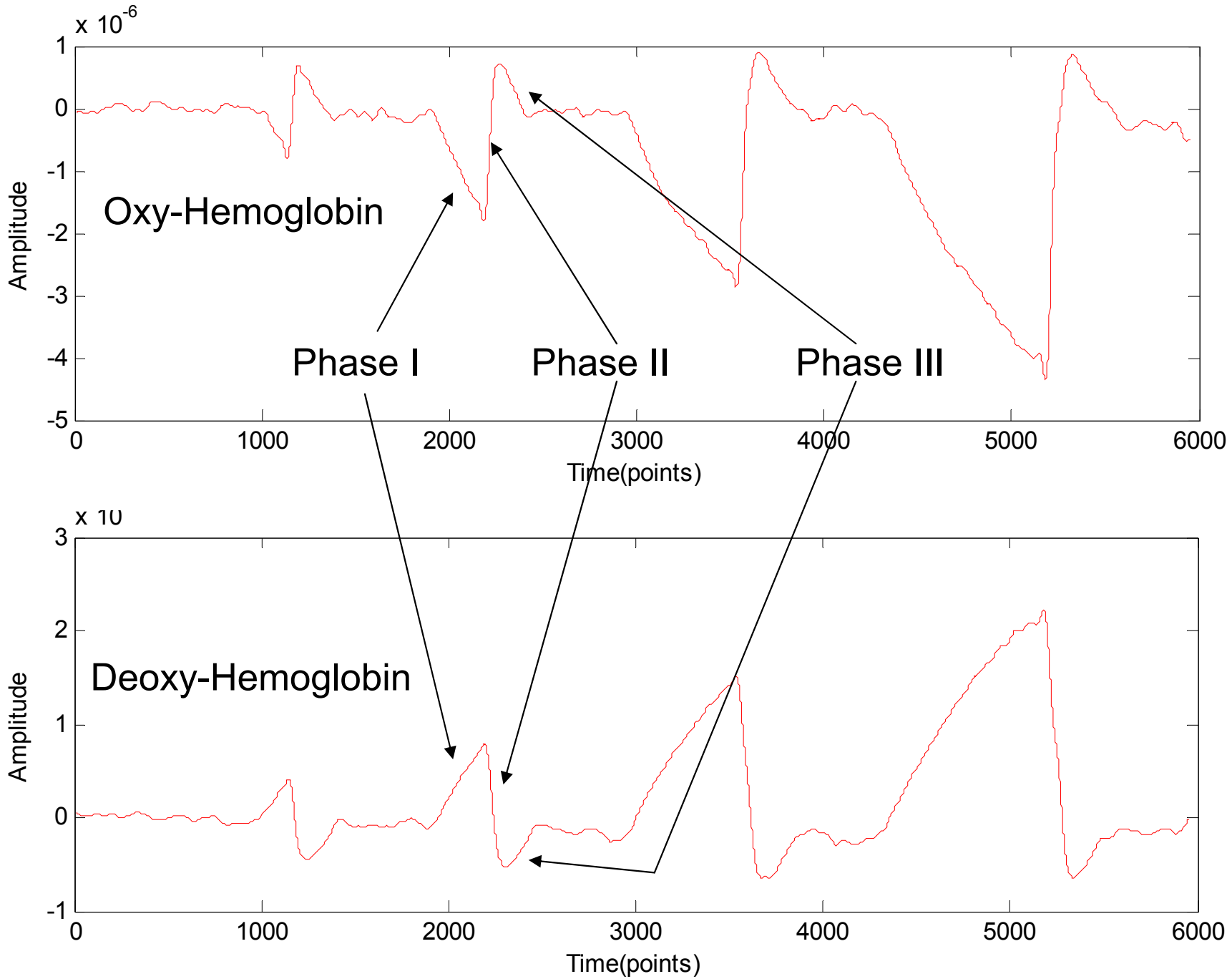
x 10^-6
1
0
-1
-2
-3
-4
-5
Amplitude
Oxy-Hemoglobin
Phase I
Phase II
Phase III
0
1000
2000
3000
4000
5000
6000
Time(points)
x 10
3
2
1
0
-1
Amplitude
Deoxy-Hemoglobin
0
1000
2000
3000
4000
5000
6000
Time(points)

Hemoglobin Fluctuations, Spatially Integrated Across Reconstructed Image

Euglycemic

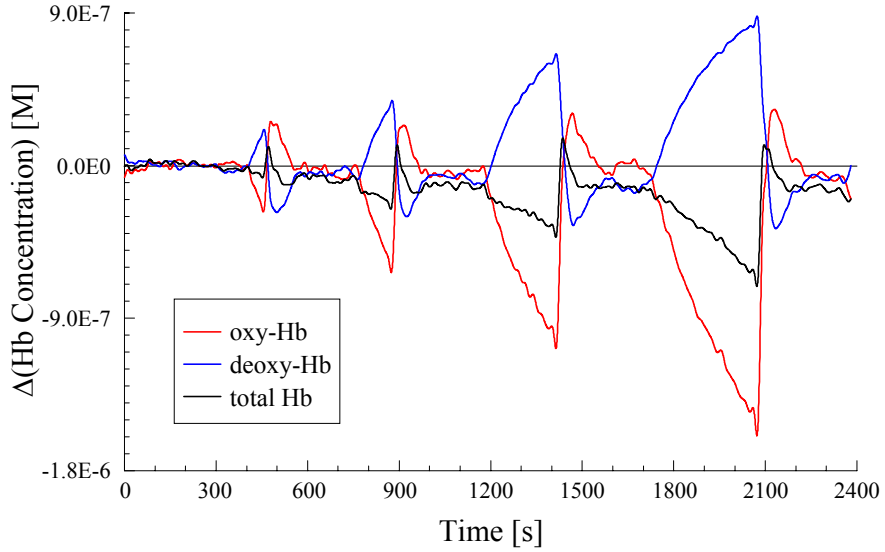

Type-2 Diabetic

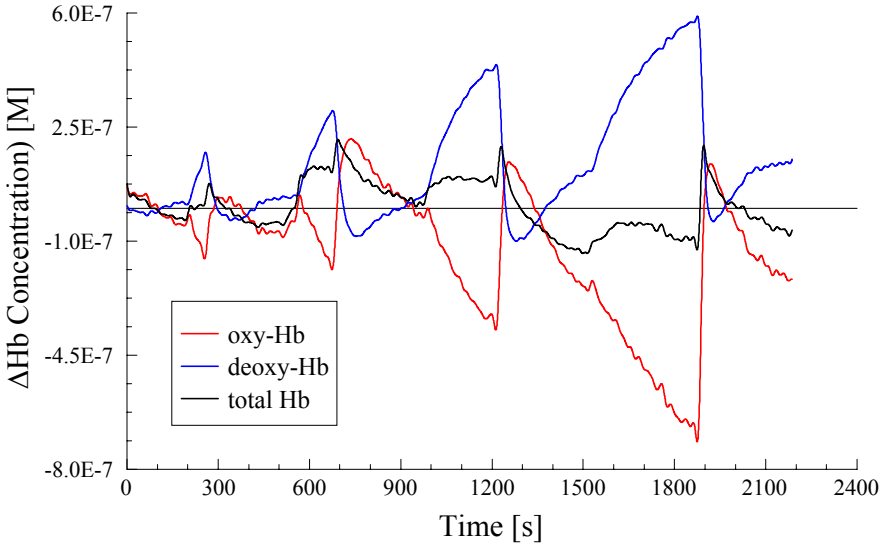

Consistency Between Detector and Image Hb Fluctuations

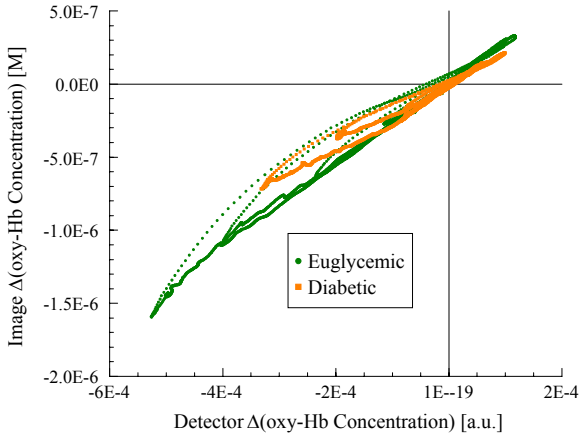

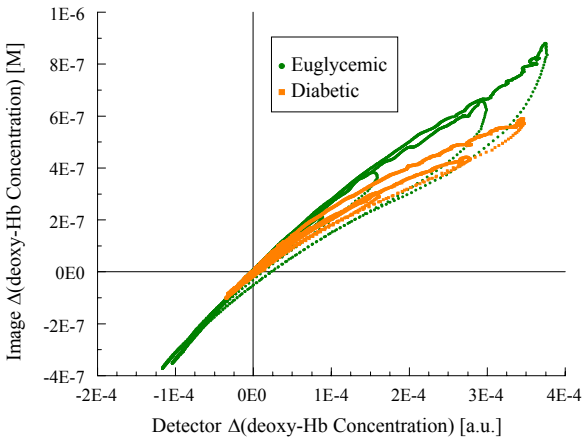

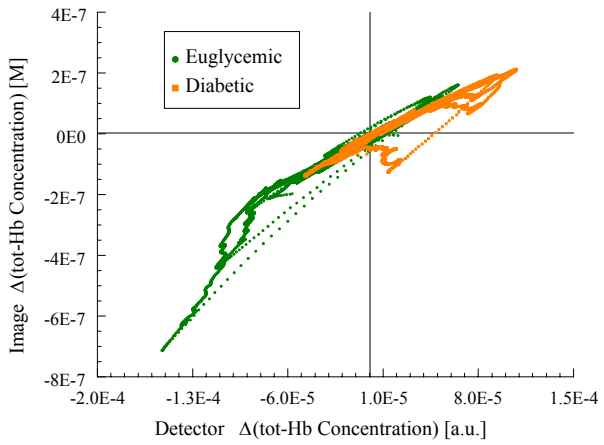

Evaluation of Peripheral Vascular Disease Using Optical Tomography

CONCLUSIONS

Time series imaging of the hemoglobin signal provides a simple and direct means of exploring vascular changes in the periphery in response to a transient hemodynamic challenge. The observed responses to induction of arterial occlusion and tissue ischemia include repeatable changes in amplitude and contrast features of the cross-sectional maps. The optical rate metrics considered are significantly correlated with physiological tissue state (i.e., whether euglycemic or poorly-controlled diabetic), suggesting that DYNOT measures of the periphery may serve as a suitable noninvasive surrogate for monitoring long-term effects of diabetes on the peripheral vasculature.

REFERENCES

[1] R. L. Barbour, H. L. Graber, Y. Pei, S. Zhong, and C. H. Schmitz, "Optical tomographic imaging of dynamic features of dense–scattering media," J. Opt. Soc. Am. A 18, 3018–3036 (2001).
[2] Arridge, S.R., 1999, "Optical Tomography in Medical Imaging," Topical Review, *Inverse Problems*, 15, R41-R93.
[3] Y. Pei, H. L. Graber, and R. L. Barbour, "Influence of systematic errors in reference states on image quality and on stability of derived information for DC optical imaging," Appl. Opt. 40 5755–5769 (2001).
[4] G. Strangman, J. P. Culver, J. H. Thompson, and D. A. Boas, "A quantitative comparison of simultaneous BOLD fMRI and NIRS recordings during functional brain activation," *Neuroimage* **17,** 719-731 (2002).
[5] R. B. Buxton, *Introduction to Functional Magnetic Resonance Imaging: Principles and Techniques*, Cambridge University Press, Cambridge, (2002).
[6] *Blood Perfusion and Microenvironment of Human Tumors*, M. Molls and P. Vaupels, Eds., Springer-Verlag, Berlin, 2000.
[7] K.B. Stansberry et al., "Impaired Peripheral Vasomotion in Diabetes," *Diabetes Care,* 19: 715-721(1996)

ACKNOWLEDGEMENT

This research was support in part by the National Institutes of Health (NIH) under Grants R21-HL67387, R21-DK63692 and R41-CA96102.